Objective Measurement of Hypertrophic Scars using Skin Colorimeter

Iveta Bryjova[1], Jan Kubicek[1], Vladimir Kasik[1], Daniel Kamensky[1], Hana Klosova[2], Marek Penhaker[1] and Martin Cerny[1]

[1]*VSB–Technical University of Ostrava, FEECS, K450, 17. Listopadu 15, Ostrava-Poruba, Czech Republic*

[2]*Burn Centre, University Hospital Ostrava, 17. Listopadu 1790 Ostrava-Poruba, Czech Republic*

Keywords: Skin Colorimeter Burns, Scars, Prototype.

Abstract: The paper deals with the methodology of the scars pigmentation objective assessment and their time evaluation on the base acquired data with the skin colorimeter prototype DSC1 (Detection of Scar Color). The analysis is primarily focused on the hypertrophic scars pigmentation assessment after heeling of deep burns which often exhibit the pigmentation. In the process of the scars evaluation in some patients it goes to the spontaneous pigmentation changes. If the pigmentation changes long-term persist and patient requires corrections, various treatment methods can influence these pigmentation changes (for instance the laser therapy and others). In the context of the complex development evaluation and in the process of the scars treatment, these changes are commonly observable well but their quantification is usually difficult, therefore using of the objective methods is desirable. The particular kind of such objective method is the skin colorimeter. The technical concept and testing of the skin colorimeter prototype DSC1 is presented in this paper.

1 INTRODUCTION

Hypertrophic scarring of burns represents the most frequent complication of the trauma, especially in the deep burns when both epidermis and dermis are destroyed. In the case of the normal circumstances, the healing process goes in three phases: inflammation, proliferation and remodelling phase. In the case of the complicated healing, the risk of developing hypertrophic, functionally restrictive and aesthetically objectionable scars is particularly high. (Blazek et al., 2015), (Cerny et al., 2008)

Hypertrophic scars develop within the primary wound and protrude over the level of the surrounding skin, they are painful, tough, itching, initially red and may progress to scarry contractures requiring surgical treatment. Deep burn scars often present also pigmentation disorders in the terms of decreased pigmentation, the so-called hypopigmentation, increased pigmentation, the so-called hyperpigmentation or a mix of different intensity thereof. The pigmentation disorders affecting the scar make it more visible against the healthy tissue which is aesthetically less acceptable for the patient. Pigmentation disorders exhibit from multiple factors and have not been clarified exactly yet. The main indications of the burns are the depth and scope of the burn, activity and duration of the inflammatory phase of healing, also various cellular mediators (NO, histamine) and other internal tissue factors which influence melanogenesis in melanocytes. At the same time certain exogenous influences enter the game, such as UV radiation. The factors mentioned above are often antagonistic, therefore, the resulting changes in the pigmentation are difficult to predict and highly individual. There are several scales for clinical evaulation: Patient and Observer Scar Assessment Scale, Visual Analog Scale, Manchester Scar Scale and the most frequently used Vancouver Scar Scale which uses pigmentation classification, elevation, pliability and vascularisation of the scar. Scar assessment using the above scales is inherently subjective – it depends upon the experience and skills of the physician performing clinical assessment. (Augustynek et al., 2010), (Scafide et al., 2016), (Shin et al., 2015), (Stekelenburg et al., 2016)

Bryjova I., Kubicek J., Kasik V., Kamensky D., Klosova H., Penhaker M. and Cerny M.
Objective Measurement of Hypertrophic Scars using Skin Colorimeter.
DOI: 10.5220/0006147101260133
In *Proceedings of the 10th International Joint Conference on Biomedical Engineering Systems and Technologies (BIOSTEC 2017)*, pages 126-133
ISBN: 978-989-758-216-5

2 STATE OF ART

Subjective methods for the evaluation of the color changes of hypertrophic scarring after burn trauma are widely described in scientific articles published in high-impact journals worldwide. Despite this fact, a objective method for burns assessment is still missing. The recent research shows that there are not many published scientific papers that would specifically focus on the objective evaluation of color hypertrophic scarring after burn injury.

Published results of clinical trials in particular describe the effect of UV radiation linked with an increasing incidence of skin cancer. In paper (Klosová et al., 2013) the authors publish the results of clinical measurements carried out on 27 male and 31 female probands, in age ranging from 6 to 9 years. The main objective of the study was to demonstrate that the incidence of skin cancer in adulthood is closely linked to the action of ultraviolet radiation in childhood. For an objective assessment of the skin color a commercial measuring device – namely, colorimeter Chroma Meter CS-200 (Konica Minolta, Japan) – was used. The results proved very high accuracy of the measurement.

In (Štětinský et al., 2015) the authors publish the results of a comparative study of two different methods of objective assessment of depigmentation using reference colorimetric methods. The measurement was performed by the colorimeter Chroma Meter CS-200 (Konica Minolta, Japan) and digital camera with polarization spectroscopic technology TiVi600 (Tissue Viability Imager TiVi600, WheelsBridge AB, Linkoping, Sweden). The results prove the fact that TiVi600 non-contact sensing achieves more accurate results than colorimeter Chroma Meter CS-200.

Another comparative study was performed with the target of evaulation the potential of selected parameters measurements (measurement accuracy, sensitivity and reproducibility) of a new commercial device Antero 3D (Miravex Limited, Ireland) with leading commercial dermatology devices Mexameter MX 18 (Courage Khazaka, Germany) and Colorimeter CL 400 (Courage Khazaka, Germany). The results of comparative analysis of these devices showed that Antero exhibits more sensitivity melanin and also improved resolution capability of erythema and melanin. The sensitivity of Mexameter and Colorimeter is almost identical.

Based on the results of the search of available commercial equipment for the detection of human skin color, or melanin concentration, we proceeded to the actual realization of the prototype skin colorimeter DSC1 order to objectify color change hypertrophic scars after thermal trauma in clinical practice. The main focus was to design a device that will be compatible and safe for clinical use, but also economically feasible.(Cerny et al., 2009), (Kukucka, 2009), (Machaj et al., 2016), (Romanelli et al., 2013), (Verhaegen et al., 2014).

3 HARDWARE DESIGN OF SKIN COLORIMETER

The functional unit of the colorimeter DSC1 is composed from several commercially available electronic components: color sensor TSC230, programming board Arduino Uno with microprocessor ATMega328 and alphanumeric LCD display 16x2. For the initial test run wiring breadboard with the Arduino kit connection cables were applied. In the first step, validation of the measuring using low-cost optical components was performed. The individual hardware parts are represented in the block diagram (fig. 1). The essential component of the device is the programmable color sensor TSC230. The sensor is able to detect any number of colours, and works on the principle of light intensity into frequency transformation. This part include 4 illuminating LED diodes in squared configuration, and the so-called RGB field (fig. 2). (Penhaker et al., 2013)

The RGB field is placed in the middle of the sensor and contains 64 quartz photodiodes. Each photodiode is equipped by 3 filters intended for the detection of red, green and blue color. 16 photodiodes are not equipped by filters, and they are primarily used for the scanning an detection of the white illumination. (Penhaker et al., 2011)

Digital input and output of the sensor is facilitated by the communication interphase with the microcontroller AVR ATMega 328 which is built in the programming board Arduino Uno. The sensor is linked with the microcontroller by six digital I/O lines which allows for picking the respective color (R/G/B), sensor sensitivity (Power down /2 % /20 % /100 %), output instruction and one pin for signal output. In the output we obtain rectangular signal (fig. 3), its frequency (AA) is given by the photodiode current. (Majernik et al., 2014), (Marek and Krejcar, 2015)

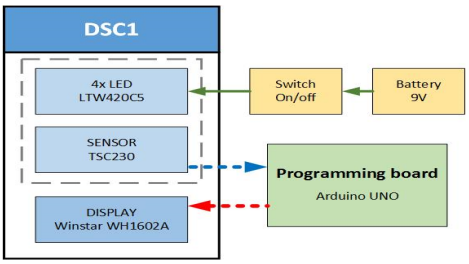

Figure 1: The block diagram of the DSC1 hardware part.

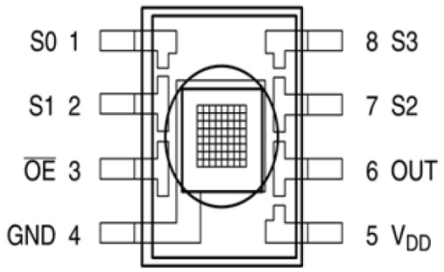

Figure 2: XY RGB photodiode field of the TSC230 sensor.

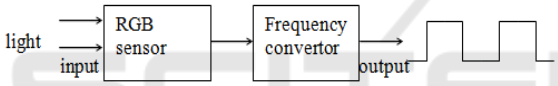

Figure 3: Principle of rectangular signal transformation.

The frequency f_0 represents the sensor detection function and is described by the following formula:

$$f_0 = f_D + (\mathrm{Re}.Ee) \quad (1)$$

where f_0 denotes the output frequency, f_D denotes the output frequency for darkness state, i.e. when $Ee = 0$ as a result leakage currents, $Ee(mW\ cm^2)$ is the intensity of the radiation incidence and $Re(kHz\ (mW/cm^2))$ denotes the sensor reaction to the wavelength of the respective light. Due to the fact that frequency f_0 is directly proportional to brightness of the individual colour components, it is possible to represent the appropriate output frequency in RGB color model and obtain the resulting colour. During the start-up it is possible to calibrate two levels in the RGB space – absolute black color is represented by zero coordinates given: [0, 0, 0] which then represents the darkness status of f_D constant, and absolute white color is given: [255, 255, 255] which denotes the maximum RGB level also called the white balance. These levels therefore define the brightness scale of the individual components of the RGB model [0 - 255]. (Augustynek and Penhaker, 2011)

After plugging-in of the sensor (fig.4) the power supply and communication with the programming board was tested. A bypassing capacitor (reduction of high frequency current flow) and a LCD display for simple viewing of the data measured were connected to the feeder circuits. We use the potentiometer (10 $k\Omega$) linked with the LCD display to adjust the required contrast. There is also push-button switch for activation of the circuit. (Penhaker et al., 2012), (Vybiral et al., 2011)

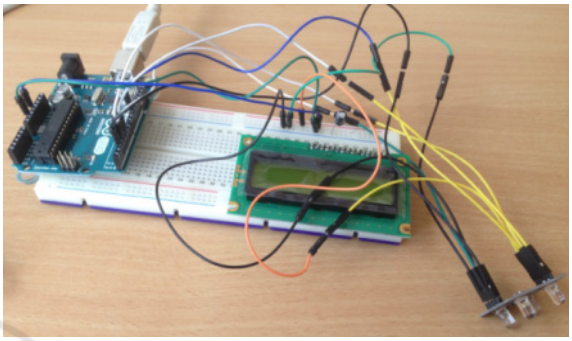

Figure 4: Testing HW connection of the sensor with the programming board.

The last step in completion of DSC1 was the design (fig. 5, 6, 7, 8) and 3D print of the protective cover to meet the hygiene requirements for the clinical use.

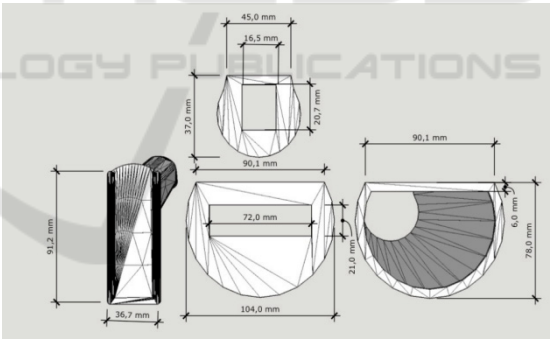

Figure 5: The protective cover – the below view.

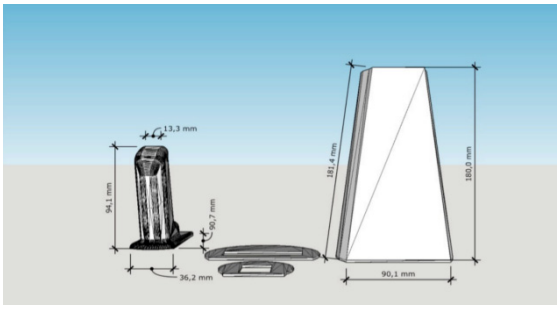

Figure 6: The protective cover – the back view.

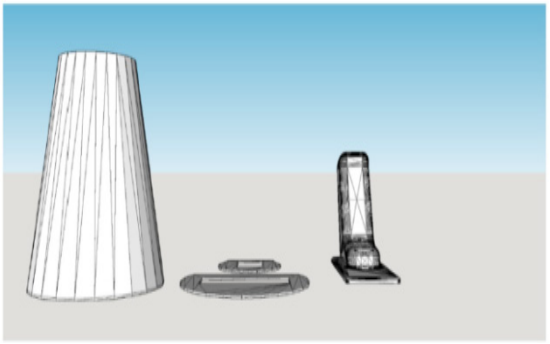

Figure 7: The protective cover – the front view.

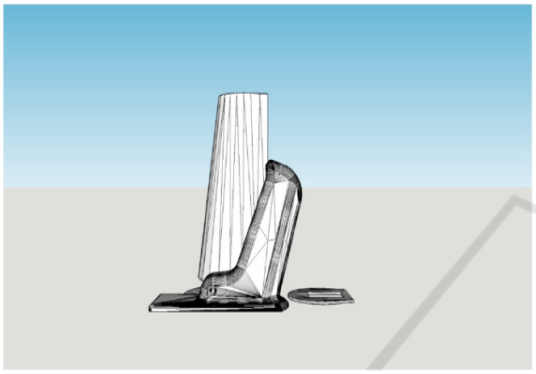

Figure 8: The protective cover – the right view.

(Kaartinen et al., 2011), (Kubicek et al., 2016), (Lammers et al., 2011).

4 SOFTWARE DESIGN OF SKIN COLORIMETER

The associated software of colorimeter prototype is designed in the JAVA language in the Arduino IDE environment, and it utilizes functionalities of the ElecFreaks library, especially functionalities for signal frequency measurement and LCD display control.

The controlling algorithm is described in the flow chart (fig.9). In the first step, the LiquidCrystal lcd() functionality and the #define clause were used to define communication pins of the LCD display and the sensor. In the consecutive step, the sensor is initialized and the frequency scale is adjusted on 2 % (enables measurement with higher sensitivity). Consequnetly, the sensor is calibrated to level [255, 255, 255] which in RGB space corresponds with the absolute white color. By this way, the upper limit of the RGB space is established. Calibration sensor is done by mat white plate or cardboard. Calibration must be done during the first start or restart. (Bryjova et al., 2016).

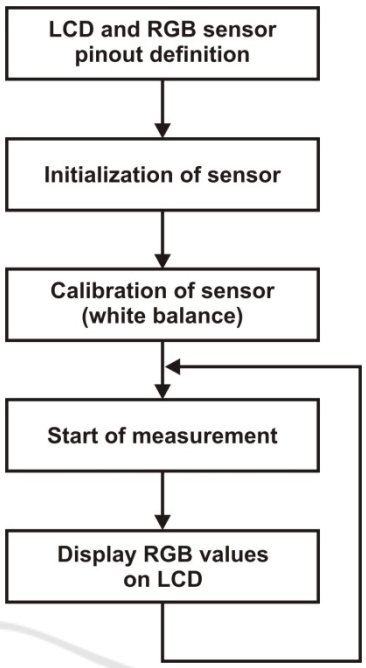

Figure 9: Algorithm flow chart of the DSC1 skin colorimeter.

5 CLINICAL TESTING AND RESULTS

Verification of the reliability and the accuracy of the device are tested on the base clinical measurements; just a few selected cases are discussed. Case 1 represents a male aged 28 with a hypertrophic scar caused by a thermic trauma (fig.10) at the dorsal side of the right arm. Altogether 10 measurements of the hypertrophic scars and the same number of control measurements of the healthy arm are performed.

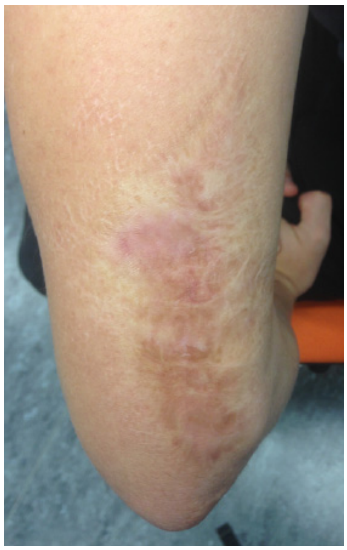

Figure 10: Arm affected by the hypertrophic scar.

The results of the measurements are summarized in the table (tab. 1) and on the scatter plot (fig. 12) for each color component R, G, B; the scatter plot moreover contains luminance calculated from color components according to the standard formula Y = 0.299R + 0.587G + 0.114B. Values representing the scars are plotted by triangles, values representing the control measurements are plotted by the circles, the individual color components and luminance are presented in corresponding colors and in black. The results are further represented by the box plot (fig. 11) showing the measurements of the scars (see the left part of the diagram) and control measurements of the healthy skin (see the right part of the diagram). These graphic outputs are supplemented by comparison of the color and luminance of the hypertrophic scar and healthy skin.

Table 1: The overview of the RGB values measured for the scary and healthy parts of the arm skin.

	scary			healthy		
measurement	R	G	B	R	G	B
1	175	53	34	190	66	38
2	172	51	33	189	63	33
3	170	59	33	186	65	36
4	175	58	32	183	63	34
5	179	59	32	199	70	60
6	179	60	34	202	71	60
7	179	60	35	192	62	38
8	179	52	32	198	68	38
9	176	58	32	197	67	37
10	179	58	33	201	67	31

Diversity of color components and luminance is statistically tested in the form of null hypothesis of equation of mean values of dependent data samples, sequentially for the color components and luminance. For testing the Location Test functionality implemented in the Mathematica software version 10.4 developed by Wolfram Research Inc. was applied which automatically selects the optimum way of testing based on pre-tests of the data samples. In this particular case, the pair Student´s t-test is selected for the red and green components and luminance and the signed rank test was used for the blue component.

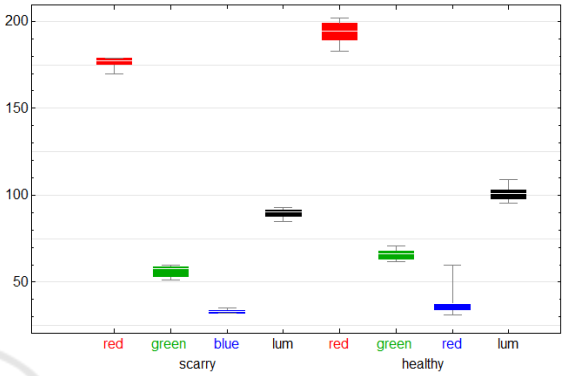

Figure 11: Box Plot – the arm affected by the hypertrophic scar.

The results are unambiguous – all the RGB components and luminance Y in the scary skin at the level of significance 0.05 are statistically significantly lower (scarry skin is darker as shown in the above comparison of colors, p-values for R, G, B and Y components being sequential 8 x 10-7, 5.2 x 10-5, 0.015 and 6.8 x 10-6.

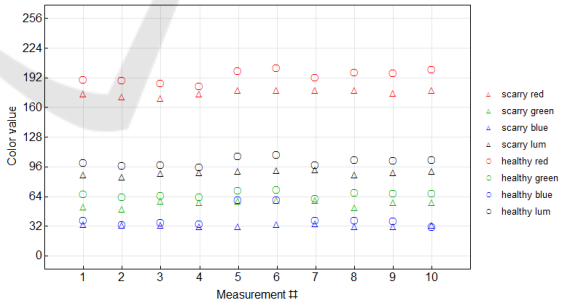

Figure 12: Scatter Plot – arm affected by the hypertrophic scar.

Case 2 is a patient hospitalized in the Burns Centre of the Teaching Hospital in Ostrava (fig. 13). The testing involved measurement of extensive mature hypertrophic scars following an injury by the electric current. The patient agreed with the measurement and signed an informed consent. The measurement is done under constant ambient conditions: temperature 22.8 °C, relative humidity 30.7 %,

patient´s body temperature 36.2 °C. Both the scarry and healthy parts of the body are tested separately 10 times. Two anatomical locations are measured (shoulder and crus).

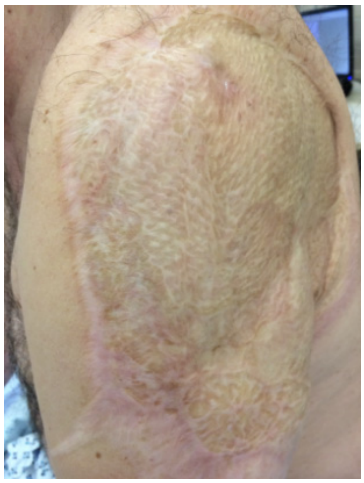

Figure 13: Affected shoulder after electrical current injury.

For the statistical imaging and testing analogical procedure is used as in the case 1. In this particular case, the pair Student´s t-test is selected for all color components as well as luminance. The results are again unambiguous – all the RGB components as well as luminance Y in the scarry skin are statistically significantly lower (scarry skin is darker as shown in the above comparison of colors, box plot (fig. 14) and scatter plot (fig. 15), p-values for R, G, B and Y components being sequentially 2.2 x 10^{-9}, 1.0 x 10^{-8}, 3.0 x 10^{-10} and 7.5 x 10^{-11}.

Table 2: Overview of the RGB values measured for the scary and healthy parts of the shoulder skin.

	scarry			healthy		
measurement	R	G	B	R	G	B
1	155	70	65	183	105	92
2	159	67	61	184	105	92
3	156	72	68	184	104	91
4	151	78	67	185	105	93
5	149	75	66	186	107	94
6	149	73	63	186	106	93
7	151	71	62	186	107	94
8	154	73	63	184	106	94
9	154	64	65	183	106	96
10	156	60	68	185	107	93

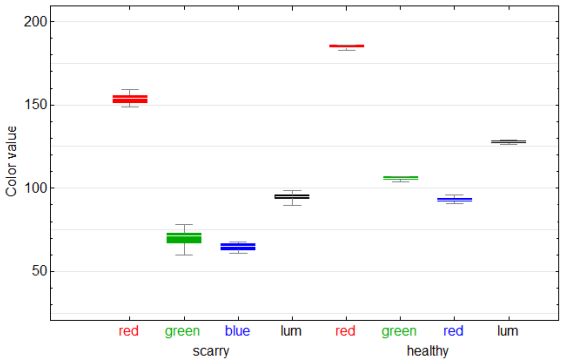

Figure 14: Box Plot – shoulder after the electrical current injury.

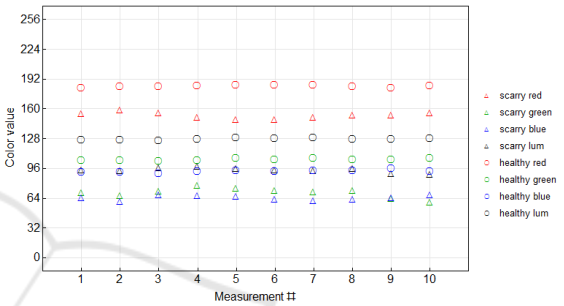

Figure 15: The Scatter Plot – the shoulder after the electrical current injury.

Left crus

Statistical imaging and testing is performed using analogical procedure as in the case 1. In this particular case, the pair Student ´s test is selected for red and green components and luminance and the signed rank test is used for the blue component. R and G color components as well as luminance Y in the scarry skin are statistically significantly lower (scarry skin is darker as shown in the above comparison of colors, box plot (fig. 17) and scatter plot (fig. 18), p-values for R, G and Y being sequentially 0.001, 0.019 and 0.012

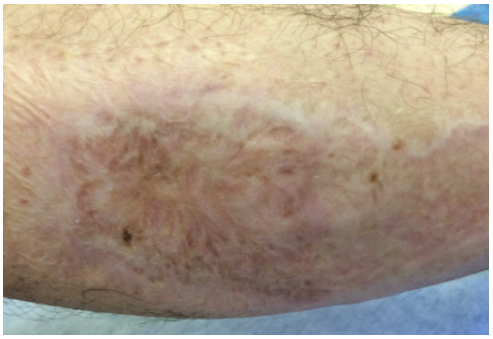

Figure 16: The crus with the hypertrophic scar.

On the contrary, in the blue component we do not reject the null hypothesis of equation of the mean value on the basis of p-value 0.437. Here, difference in luminance is less obvious though noticeable even when observing and comparing colors by naked eye.

Table 3: Overview of the RGB values measured for the scary and healthy parts of the crus skin.

	scarry			healthy		
measurement	R	G	B	R	G	B
1	121	57	35	134	76	69
2	128	71	67	137	76	69
3	128	71	67	137	76	69
4	128	72	68	137	77	66
5	130	72	68	141	78	71
6	130	72	68	138	77	67
7	123	68	65	135	74	67
8	123	69	65	130	71	64
9	126	71	68	121	68	63
10	129	72	67	133	73	67

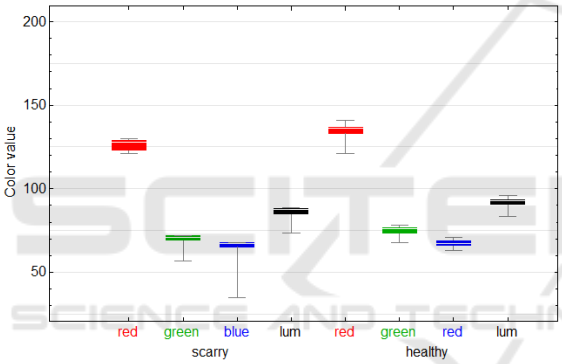

Figure 17: Box Plot – the crus with the hypertrophic scar.

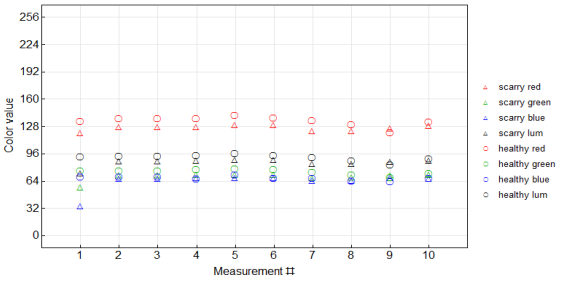

Figure 18: Scatter Plot – the crus with the hypertrophic scar.

6 CONCLUSIONS

Testing results prove that areas containing scars are statistically significantly darker than the normal skin, and it all them color components, including the luminance. There is a one exception. Just in the case of the left crus the blue scar component is insignificantly darker. The proposed prototype of the skin colorimeter DSC1 seems to be promising device in the context of the objective assessment of the color skin weaker differences (hypertrophic and other scars) in the clinical conditions.

The device primarily allows for the quantification of the pigmentation level of the hypertrophic scars as the consequence after extensive thermally traumas. In the context of the future clinical measurements the next physical and other conditions will be determined for valid values measurement which consequently will be able to represent and assess the correlation with the most frequently used clinical scale VSS (Vencouver Scar Scale).

The next steps should be focused to the miniaturization and improving of the hardware components of the DSC1. These improvements are necessary to routine using of the DSC1 for the clinical measurement as affordable, reliable and accurate method.

ACKNOWLEDGEMENT

This article has been supported by financial support of TA ČR, PRE SEED Fund of VSB-Technical univerzity of Ostrava/TG01010137. The work and the contributions were supported by the project SV4506631/2101 'Biomedicínské inženýrské systémy XII'.

REFERENCES

Augustynek, M., Labza, Z., Penhaker, M., Korpas, D., & Society, I. C. (2010). *Verification of set up dual-chamber pacemaker electrical parameters*. 2010 Second International Conference on Computer Engineering and Applications: Iccea 2010, Proceedings, Vol 2, 168-172. doi:10.1109/iccea.2010.187.

Augustynek, M., & Penhaker, M. (2011). *Non invasive measurement and visualizations of blood pressure*. Elektronika Ir Elektrotechnika(10), 55-58. doi:10.5755/j01.eee.116.10.880.

Blazek, P., Krenek, J., Kuca, K., Krejcar, O., Jun, D., & Ieee. (2015). *The biomedical data collecting system.* 2015 25th International Conference Radioelektronika (Radioelektronika), 419-422.

Bryjova, I., Kubicek, J., Dembowski, M., Kodaj, M., Penhaker, M. 2016. *Reconstruction of 4D CTA brain perfusion images using transformation methods*, Advances in Intelligent Systems and Computing, 423, pp. 203-211.

Cerny, M., Martinak, L., Penhaker, M., & Rosulek, M. (2008). *Design and implementation of textile sensors for biotelemetry applications*. In A. Katashev, Y. Dekhtyar, & J. Spigulis (Eds.), 14th nordic-baltic conference on biomedical engineering and medical physics (Vol. 20, pp. 194-197).

Cerny, M., & Penhaker, M. (2009). *Circadian rhythm monitoring in homecare systems*. In C. T. Lim & J. C. H. Goh (Eds.), 13th international conference on biomedical engineering, vols 1-3 (Vol. 23, pp. 950-953).

Kaartinen, I.S., Välisuo, P.O., Bochko, V., Alander, J.T., Kuokkanen, H.O. 2011. *How to assess scar hypertrophy - A comparison of subjective scales and Spectrocutometry: A new objective method.* Wound Repair and Regeneration, 19 (3), pp. 316-323.

Klosová, H., Štětinský, J., Bryjová, I., Hledík, S., and Klein, L. 2013. *Objective evaluation of the effect of autologous platelet concentrate on post-operative scarring in deep burns*. *Burns*.,s. -. DOI: 10.1016/j.burns.2013.01.020.

Kubicek, J., Bryjova, I., Penhaker, M. 2016. *Macular lesions extraction using active appearance method* Lecture Notes of the Institute for Computer Sciences, Social-Informatics and Telecommunications Engineering, LNICST, 165, pp. 438-447.

Kubicek, J., Bryjova, I., Penhaker, M., Kodaj, M., Augustynek, M. 2016. *Extraction of myocardial fibrosis using iterative active shape method* Lecture Notes in Computer Science (including subseries Lecture Notes in Artificial Intelligence and Lecture Notes in Bioinformatics), 9621, pp. 698-707.

Kukucka, M. (2009). *Modeling of logic diagnostic system knowledge base evaluation*.

Lammers, G., Verhaegen, P.D.H.M., Ulrich, M.M.W., Schalkwijk, J., Middelkoop, E., Weiland, D., Nillesen, S.T.M., Van Kuppevelt, T.H., Daamen, W.F. 2011. *An overview of methods for the in vivo evaluation of tissue-engineered skin constructs* Tissue Engineering - Part B: Reviews, 17 (1), pp. 33-55.

Machaj, J., Brida, P., & Benikovsky, J. (2016). *Scalability optimization of seamless positioning service*. Mobile Information Systems. doi:10.1155/2016/9714080

Majernik, J., Jarcuska, P., & Ieee. (2014). *Web-based delivery of medical education contents used to facilitate learning of infectology subjects*. 2014 10th International Conference on Digital Technologies (Dt), 225-229.

Marek, T., & Krejcar, O. (2015). *Optimization of 3d rendering in mobile devices*. In M. Younas, I. Awan, & M. Mecella (Eds.), Mobile web and intelligent information systems (Vol. 9228, pp. 37-48).

Penhaker, M., Darebnikova, M., & Cerny, M. (2011). *Sensor network for measurement and analysis on medical devices quality control*. In J. J. Yonazi, E. Sedoyeka, E. Ariwa, & E. ElQawasmeh (Eds.), E-technologies and networks for development (Vol. 171, pp. 182-196).

Penhaker, M., Klimes, P., Pindor, J., & Korpas, D. (2012). *Advanced intracardial biosignal processing*. In A. Cortesi, N. Chaki, K. Saeed, & S. Wierzchon (Eds.), Computer information systems and industrial management (Vol. 7564, pp. 215-223).

Penhaker, M., Kasik, V., & Snasel, V. (2013). *Biomedical distributed signal processing and analysis*. In K. Saeed, R. Chaki, A. Cortesi, & S. Wierzchon (Eds.), Computer information systems and industrial management, cisim 2013 (Vol. 8104, pp. 88-95).

Scafide, K.N., Sheridan, D.J., Taylor, L.A., Hayat, M.J. 2016. *Reliability of tristimuluscolourimetry in the assessment of cutaneous bruise colour* Injury, 47 (6), pp. 1258-1263.

Shin, J.U., Kang, S.-W., Jeong, J.J., Nam, K.-H., Chung, W.Y., Lee, J.H. 2015. *Effect of recombinant human epidermal growth factor on cutaneous scar quality in thyroidectomy patients* Journal of Dermatological Treatment, 26 (2), pp. 159-164.

Stekelenburg, C.M., Hiddingh, J.,Kuipers, H.C., Middelkoop, E.,Nieuwenhuis, M.K., Polinder, S., Van Baar, M.E. 2016. *Cost-effectiveness of laser doppler imaging in burn care in The Netherlands: A randomized controlled trial* Plastic and Reconstructive Surgery, 137 (1), pp. 166e-176e.

Štětinský, J., Klosová, H., Kolářová, H., Šalounová, D., Bryjová, I. and Hledík, S. 2015. *The time factor in the LDI (Laser Doppler Imaging) diagnosis of burns*. *Lasers in Surgery and Medicine*. 47(2): 196-202. DOI: 10.1002/lsm.22291. ISBN 10.1002/lsm.22291. ISSN 01968092.

Romanelli, M., Dini, V., Mani, R. Skin and vascular assessments 2013. *Measurements in Wound Healing*: Science and Practice, pp. 193-223.

Kubicek, J., Penhaker, M., Bryjova, I., Augustynek, M. 2016. *Classification method for macular lesions using fuzzy thresholding method*) IFMBE Proceedings, 57, pp. 239-244.

Verhaegen, P.D.H.M., Bloemen, M.C.T., Van Der Wal, M.B.A., Vloemans, A.F.P.M., Tempelman, F.R.H., Beerthuizen, G.I.J.M., Van Zuijlen, P.P.M. 2014. *Skin stretching for primary closure of acute burn wounds* Burns, 40 (8), pp. 1727-1737.

Vybiral, D., Augustynek, M., & Penhaker, M. (2011). *Devices for position detection*. Journal of Vibroengineering, 13(3), 531-535.